

# Magnetization plateau in the frustrated quantum spin system $\text{Cs}_2\text{CuBr}_4$

T. Ono,<sup>1,\*</sup> H. Tanaka,<sup>1,†</sup> H. Aruga Katori,<sup>2</sup> F. Ishikawa,<sup>3</sup> H. Mitamura,<sup>3</sup> and T. Goto<sup>3</sup>

<sup>1</sup>Department of Physics, Tokyo Institute of Technology, Meguro-ku, Tokyo 152-8551, Japan

<sup>2</sup>RIKEN (The Institute of Physical and Chemical Research), Wako, Saitama 351-0198, Japan

<sup>3</sup>Institute for Solid State Physics, The University of Tokyo, Kashiwanoha, Kashiwa, Chiba 277-8581, Japan

(Received 28 August 2002; published 31 March 2003)

The magnetic phase transitions of  $\text{Cs}_2\text{CuBr}_4$ , which may be described as a spin- $\frac{1}{2}$  quasi-two-dimensional frustrated antiferromagnet, were investigated by means of magnetization and specific heat measurements.  $\text{Cs}_2\text{CuBr}_4$  undergoes magnetic ordering at a Néel temperature  $T_N = 1.4$  K at zero magnetic field. The magnetization curve has a plateau at approximately one-third of the saturation magnetization for a magnetic field  $H$  parallel to the  $b$  and  $c$  axes, while no plateau was observed for  $H \parallel a$ . The field-induced phase transition to the plateau state appears to be of first order. The magnetization plateau should be attributed to quantum fluctuation. The magnetic field vs temperature diagram is presented.

DOI: 10.1103/PhysRevB.67.104431

PACS number(s): 75.10.Jm, 75.25.+z, 75.30.Kz, 75.45.+j

## I. INTRODUCTION

In triangular antiferromagnets (TAFs), spin frustration produces a rich variety of phase transitions.<sup>1</sup> For a two-dimensional (2D) classical Heisenberg TAF or a ferromagnetically stacked classical Heisenberg TAF, the spin structure of the ground state in a magnetic field cannot be uniquely determined. This is because the number of parameters which determines the spin configuration is more than the number of equations giving the equilibrium condition. Thus the ground state exhibits a continuous degeneracy in the magnetic field, and no phase transition accompanied by the anomaly of magnetization arises up to saturation, so the magnetization curve is monotonic.

For the quantum Heisenberg model on a 2D or ferromagnetically stacked triangular lattice, the quantum fluctuation plays an important role in determining the spin structure of the ground state. The quantum fluctuation can remove the continuous degeneracy of the ground state. In the spin wave theory which represents the spin system as a harmonic oscillator, the quantum fluctuation is expressed by zero-point oscillation. Since the zero-point oscillation energy  $\sum_{\mathbf{Q}} \frac{1}{2} \hbar \omega(\mathbf{Q})$  depends on the spin structure, one spin structure with the lowest zero-point oscillation energy can be stabilized. The zero-point oscillation energy varies with the magnetic field, so phase transition can occur in magnetic fields.<sup>2,3</sup>

The magnetization process in the 2D Heisenberg TAF has been investigated theoretically by many authors.<sup>4-6</sup> It was demonstrated that the up-up-down (*uud*) spin structure illustrated in Fig. 1(b) is stabilized in a finite field range, so that

the magnetization curve has a plateau at one-third of the saturation magnetization  $M_s$ . The magnetization plateau attracts the interest as a macroscopic quantum phenomenon. Figure 2 shows the schematic magnetization curve for the 2D Heisenberg TAF.  $H_{c1}$  and  $H_{c2}$  are the lower and upper edge fields, respectively, and  $H_s$  is the saturation field. The two coplanar structures illustrated in Figs. 1(a) and 1(c) are stabilized for  $H < H_{c1}$  and  $H_{c2} < H < H_s$ , respectively. The highly symmetric umbrella structure illustrated in Fig. 1(d) is not optimal.

The field-induced phase transition caused by the quantum fluctuation was actually observed in a ferromagnetically stacked TAF,  $\text{CsCuCl}_3$ .<sup>7-9</sup> In the ordered state below  $T_N = 10.5$  K, spins lie in the  $c$  plane due to the small easy-plane anisotropy and form the  $120^\circ$  structure.<sup>10</sup> When the magnetic field is applied along the  $c$  axis,  $\text{CsCuCl}_3$  undergoes a phase transition at  $H_c \sim 12$  T accompanied with a small magnetization jump.<sup>7,11,12</sup> Nikuni and Shiba<sup>2</sup> demonstrated theoretically that the field-induced transition arises due to competition between the small easy-axis anisotropy and the quantum fluctuation, and that the umbrella structure stabilized by the easy-axis anisotropy changes to the high-field coplanar structure illustrated in Fig. 1(c), skipping structures (a) and (b). Their theory was confirmed by a neutron scattering experiment in pulsed high magnetic fields.<sup>8</sup> However, the experimental realization of the quantum-fluctuation-assisted plateau at  $\frac{1}{3}M_s$  has not been reported to date.

Cesium tetrabromocuprate(II)  $\text{Cs}_2\text{CuBr}_4$  has an orthorhombic structure with space group  $Pnma$ .<sup>13,14</sup> Figure 3(a) shows the perspective view of the crystal structure along the

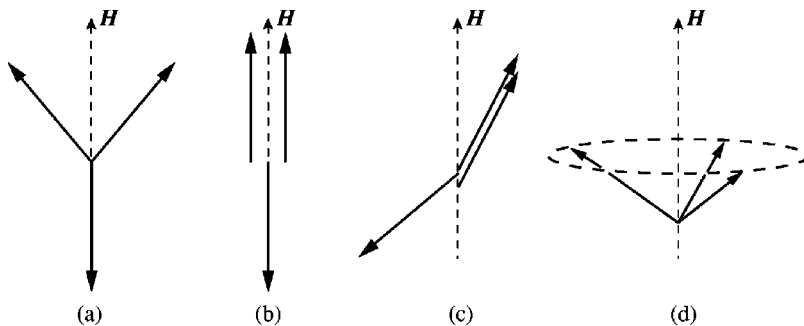


FIG. 1. Spin structures of a 2D triangular antiferromagnet in a magnetic field. (a) Low-field coplanar structure. (b) Collinear structure. (c) High-field coplanar structure. (d) Umbrella structure.

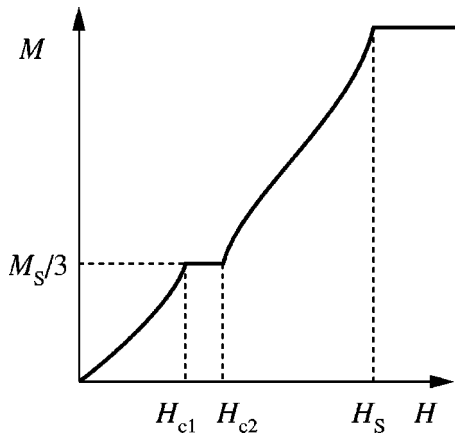


FIG. 2. Schematic magnetization curve for the 2D Heisenberg triangular antiferromagnet.

$b$  axis. Thin solid lines denote the chemical unit cell. The structure is composed of  $\text{CuBr}_4^{2-}$  tetrahedra and  $\text{Cs}^+$  ions. The tetrahedra are linked along the  $b$  axis. Because of the Jahn-Teller effect, the  $\text{CuBr}_4^{2-}$  tetrahedra are compressed along the axes perpendicular to the  $b$  axis. Figure 3(b) shows the arrangement of the  $\text{CuBr}_4^{2-}$  tetrahedra in the  $bc$  plane.

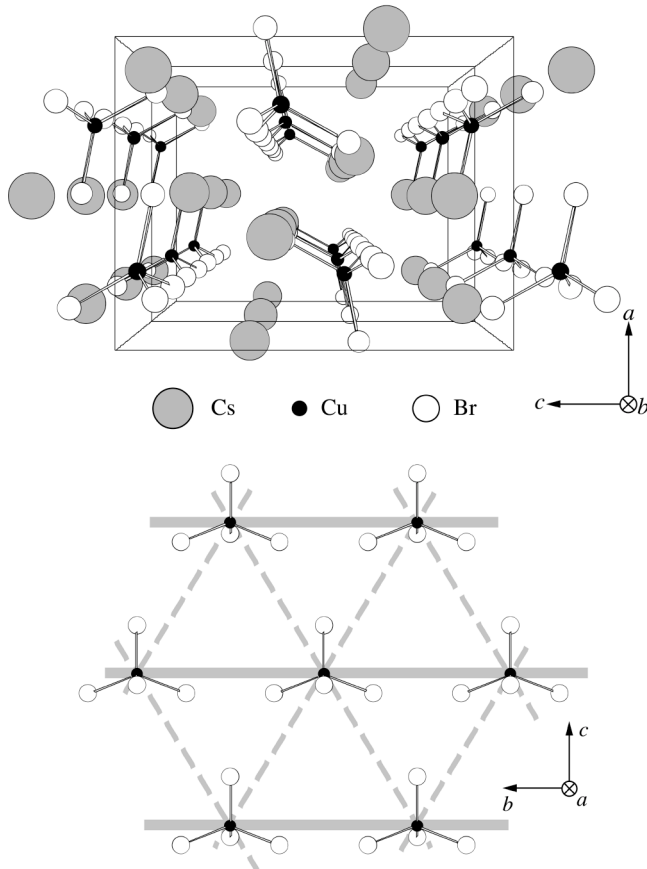


FIG. 3. (a) Perspective view of the crystal structure of  $\text{Cs}_2\text{CuBr}_4$  parallel to the  $b$  axis. Shaded, closed, and open circles denote  $\text{Cs}^+$ ,  $\text{Cu}^{2+}$ , and  $\text{Br}^-$  ions, respectively. (b) Arrangement of the  $\text{CuBr}_4^{2-}$  octahedra in the  $bc$  plane.  $\text{Cs}^+$  ions are omitted.

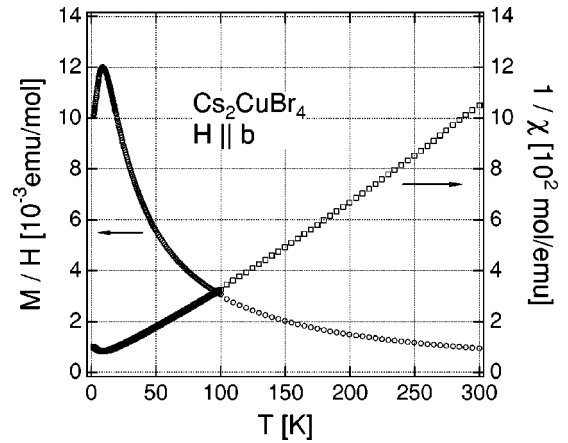


FIG. 4. Magnetic susceptibility and inverse susceptibility in  $\text{Cs}_2\text{CuBr}_4$  as a function of temperature for  $H$  parallel to the  $b$  axis.

$\text{Cu}^{2+}$  ions with spin- $\frac{1}{2}$  form a distorted triangular lattice in the  $bc$  plane. Little is known of the magnetic properties of  $\text{Cs}_2\text{CuBr}_4$ . Since the magnitude of spin is  $\frac{1}{2}$  and the exchange interactions  $J_1$  and  $J_2$  should be antiferromagnetic as observed in the isostructural  $\text{Cs}_2\text{CuCl}_4$ ,<sup>17</sup> a magnetic behavior caused by the interplay of the spin frustration and the quantum fluctuation is expected to occur in  $\text{Cs}_2\text{CuBr}_4$ . As described below, the magnetization plateau was observed.

## II. EXPERIMENTAL PROCEDURES

Single crystals of  $\text{Cs}_2\text{CuBr}_4$  were grown by the slow evaporation of aqueous solution of  $\text{CsBr}$  and  $\text{CuBr}_2$  in the mole ratio 2:1. We also prepared single crystals by the Bridgman method from the melt of a mixture of  $\text{CsBr}$  and  $\text{CuBr}_2$  sealed in an evacuated quartz tube. The crystals obtained were identified to be  $\text{Cs}_2\text{CuBr}_4$  by x-ray powder diffraction. The crystal was cleaved along the  $(0, 0, 1)$  plane. The relationship between the crystal shape and the principal axes was checked by neutron diffraction. On the  $(0, 0, 1)$  and  $(0, 1, 1)$  planes of crystals, many lines parallel to the  $a$  axis were observed. The specific heat measurements for a single crystal of  $\text{Cs}_2\text{CuBr}_4$  were carried out at RIKEN down to 0.5 K in magnetic fields up to 12 T using the microcalorimeter Oxford Instruments Mag Lab<sup>HC</sup> in which the relaxation method was employed.

The magnetizations were measured at TIT down to 1.8 K in magnetic fields up to 7 T using a superconducting quantum interference device magnetometer (Quantum Design MPMS XL). The high-field magnetization measurement was performed using an induction method with a multilayer pulse magnet at the Ultra-High Magnetic Field Laboratory, Institute for Solid State Physics, The University of Tokyo. Magnetization data were collected at  $T=0.4, 0.65,$  and  $1.6$  K in magnetic fields up to 35 T.

## III. RESULTS AND DISCUSSION

Figure 4 shows the magnetic susceptibility  $M/H$  and the inverse susceptibility in  $\text{Cs}_2\text{CuBr}_4$  as a function of temperature measured at  $H=1.0$  T for  $H\parallel b$ . With decreasing tem-

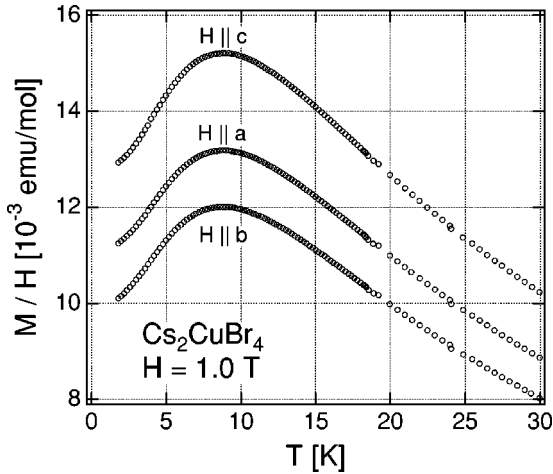


FIG. 5. Low-temperature magnetic susceptibilities in  $\text{Cs}_2\text{CuBr}_4$  for  $H$  parallel to the  $a$ ,  $b$ , and  $c$  axes.

perature, the susceptibility increases rapidly and has a broad maximum at  $T_{\text{max}} \approx 9\text{K}$ , which is characteristic of the low-dimensional antiferromagnetic spin system. However, the inverse susceptibility is a convex function of temperature and has no linear part obeying the Curie-Weiss law. This susceptibility behavior was also observed for  $H\|a$  and  $H\|c$ . As shown below, this is not due to the dominant exchange interaction being ferromagnetic.

To understand the magnetic properties of  $\text{Cs}_2\text{CuBr}_4$ , it is important to consider the crystal field acting on  $\text{Cu}^{2+}$  and its orbital state. The electronic ground state of the  $\text{Cu}^{2+}$  ion with the  $3d^9$  configuration is  ${}^2D$ . In a cubic tetrahedral crystal field, the electronic ground state splits into triply degenerate  $T_{2g}$  and doubly degenerate  $E_g$  states. The  $T_{2g}$  state has a lower energy. In the presence of the additional tetragonal crystal field due to the tetragonal distortion of the  $\text{CuBr}_4^{2-}$  tetrahedron and the spin-orbit coupling, the  $T_{2g}$  state splits into three states. The ground state is nondegenerate, so that the orbital moment is quenched. Consequently, the magnetic moment is approximately given by spin only, i.e.,  $S = \frac{1}{2}$ , which can be confirmed from the value of saturation magnetization  $M_s \approx 1\mu_B$ , as shown below. However, in general, splitting energy between the ground state and the two excited states is not much greater than room temperature, in contrast to the case of the octahedral crystal field for which splitting energy is of the order of  $10^4$  K. Although we do not know the details of splitting in the present system, we consider that the rapid decrease of the magnetic susceptibility with temperature arises from the contribution of the excited orbital states, which suppresses the effective magnetic moment.

The low-temperature susceptibilities for  $H\|a$ ,  $H\|b$ , and  $H\|c$  are shown in Fig. 5. The susceptibilities for these three different field directions exhibit similar temperature variations. No anomaly indicative of phase transition was observed down to 1.8 K. The differences between the absolute values of the three susceptibilities are due to the anisotropy of the  $g$  factor. The value of  $T_{\text{max}} \approx 9$  K for  $\text{Cs}_2\text{CuBr}_4$  is about three times as large as  $T_{\text{max}} \sim 3\text{K}$  for isostructural  $\text{Cs}_2\text{CuCl}_4$ .<sup>15</sup> This implies that the exchange interactions in  $\text{Cs}_2\text{CuBr}_4$  are larger than those in  $\text{Cs}_2\text{CuCl}_4$ .

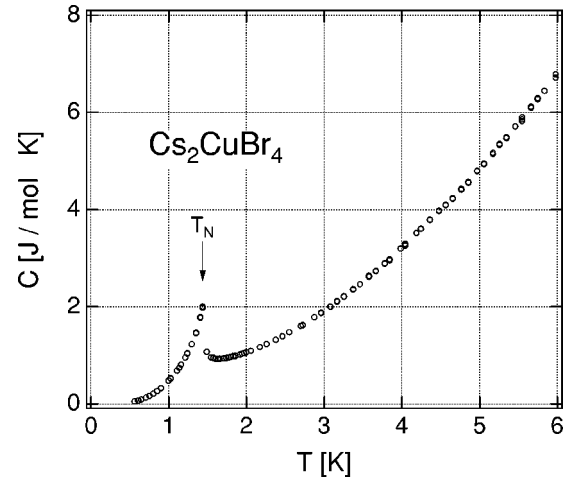


FIG. 6. The total specific heat  $C$  in  $\text{Cs}_2\text{CuBr}_4$  measured at zero field.

Figure 6 shows the total specific heat  $C$  in  $\text{Cs}_2\text{CuBr}_4$  at zero field. The  $\lambda$ -like anomaly indicative of phase transition is observed at  $T_N = 1.4$  K. The ordering temperature  $T_N$  for  $\text{Cs}_2\text{CuBr}_4$  is more than twice as high as  $T_N = 0.62$  K for isostructural  $\text{Cs}_2\text{CuCl}_4$ .<sup>16</sup> Figure 7 shows the specific heat measured at various magnetic fields for  $H\|a$ ,  $H\|b$ , and  $H\|c$ . For  $H\|b$  and  $H\|c$ , the transition temperature  $T_N$  decreases monotonically with increasing magnetic field, while for  $H\|a$ ,  $T_N$  decreases up to 8 T and then increases. In Fig. 8, the phase transition temperatures determined from the specific heat measurements are plotted.

Figure 9 shows the magnetization curves measured at  $T = 0.4$  K for  $H\|a$ ,  $b$ , and  $c$ . The data were taken in sweeping up magnetic field. Due to the mechanical noise inevitable in the pulsed high magnetic field measurement, the data taken in sweeping up and down the magnetic field do not coincide with each other. However, intrinsic hysteresis was not observed in the magnetization curves. The magnetization saturates at  $H_s \approx 30$  T. The value of the saturation magnetization, which is slightly larger than  $1\mu_B$ , is consistent with the condition that the orbital moment is quenched, and the magnetic moment is approximately given by spin only. Thus the low-temperature magnetic properties of  $\text{Cs}_2\text{CuBr}_4$  can be described by a spin- $\frac{1}{2}$  Heisenberg model with small anisotropy. The differences between the absolute values of the saturation fields and the saturation magnetizations for the three different field directions should be due to the anisotropy of the  $g$  factor.

The magnetization curve for  $H\|a$  is monotonic up to saturation, while the magnetization curves for  $H\|b$  and  $c$  have a plateau at approximately one-third of the saturation magnetization  $M_s$ . The inset in Fig. 9 shows  $dM/dH$  versus  $H$  around the magnetization plateau for  $H\|b$  and  $H\|c$ . The level of the plateau is exactly  $M_s/3$  for  $H\|b$ , while it is slightly lower than  $M_s/3$  for  $H\|c$ . The plateau region is narrow, and its field range is about 1.5 T for  $H\|b$  and 1 T for  $H\|c$ . Figure 10 shows the magnetization curve and  $dM/dH$  versus  $H$  for  $H\|b$  measured in magnetic fields up to 20 T. Since the highest field is 20 T, mechanical noise and the increase of temperature are significantly suppressed, so that

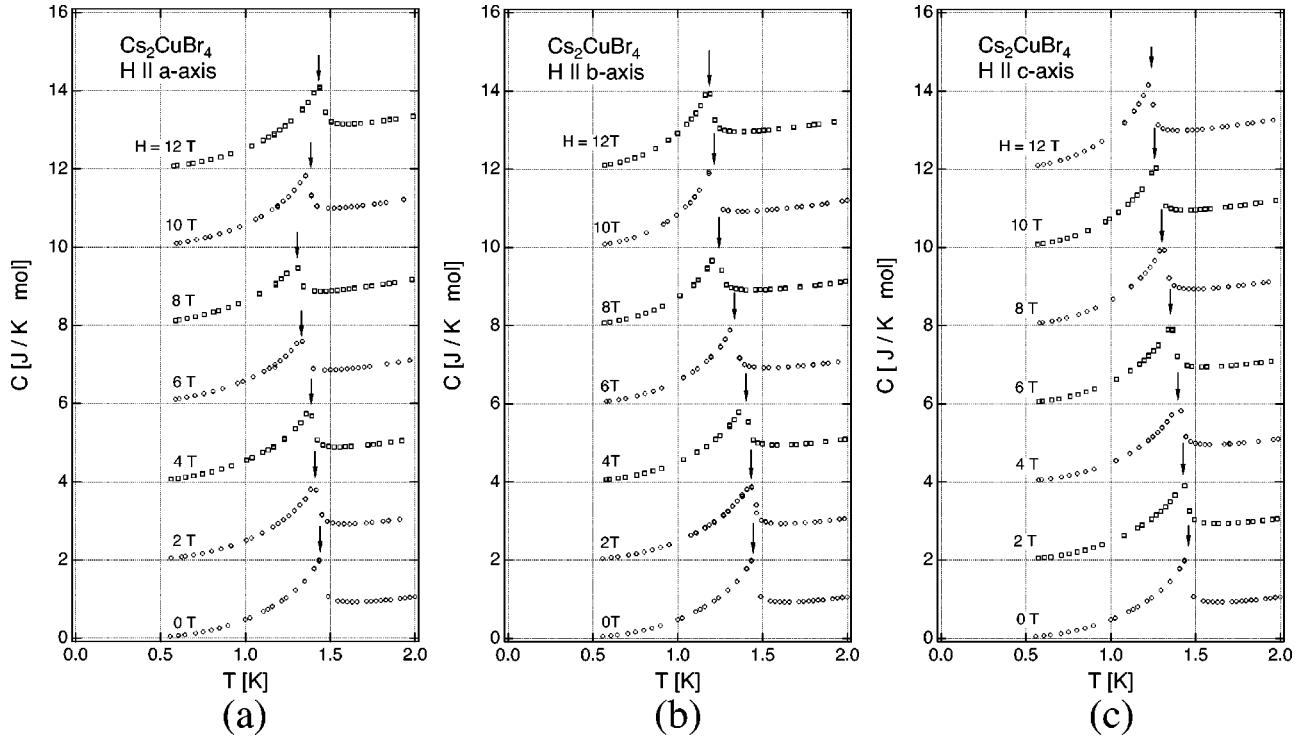


FIG. 7. The total specific heat  $C$  in  $\text{Cs}_2\text{CuBr}_4$  measured at various magnetic fields for (a)  $H \parallel a$ , (b)  $H \parallel b$ , and (c)  $H \parallel c$ . The values of the specific heat are shifted upward by  $2J/\text{mol K}$  with increasing external field.

the plateau is clearly observed. Since the field derivative of magnetization  $dM/dH$  exhibits sharp peaks at both edges of the plateau and has no tail in the slope region, the transition between the slope and the plateau regions appears to be of the first order. We also measured the magnetization process at  $T = 1.6$  K which is higher than  $T_N$ . No magnetization plateau was observed, as shown in Fig. 11. Thus we can conclude that the plateau exists only in the ordered phase.

Next we discuss our present results. The magnetic properties of isostructural  $\text{Cs}_2\text{CuCl}_4$  have been extensively investigated by magnetic susceptibility and neutron scattering experiments.<sup>15–19</sup>  $\text{Cs}_2\text{CuCl}_4$  undergoes a magnetic phase transition at  $T_N = 0.62$  K.<sup>16</sup> In the ordered phase below  $T_N$ , spins lie in a plane that is almost parallel to the  $bc$  plane and form a helical incommensurate structure with ordering vector  $\mathbf{Q}_0 = (0, 0.528, 0)$ .<sup>20</sup> The incommensurate spin structure arises from the spin frustration on the distorted triangular lattice in the  $bc$  plane [see Fig. 3(b)]. By means of neutron inelastic scattering,<sup>17–19</sup> it was demonstrated that the exchange interactions  $J_1$  and  $J_2$  are dominant and interlayer coupling is smaller than  $10^{-2} \times J_1$ . Thus  $\text{Cs}_2\text{CuCl}_4$  was characterized as a quasi-two-dimensional (2D) frustrated spin system.

Because the crystal structures of  $\text{Cs}_2\text{CuBr}_4$  and  $\text{Cs}_2\text{CuCl}_4$  are the same, we can expect that  $\text{Cs}_2\text{CuBr}_4$  is also a quasi-2D frustrated spin system. Quite recently, we performed neutron elastic scattering in  $\text{Cs}_2\text{CuBr}_4$  for the scattering vector in the  $a^*b^*$  plane.<sup>21</sup> The magnetic Bragg reflections were observed at  $\mathbf{Q} = (h, k \pm 0.575, 0)$ , with integer values of  $h$  and  $k$ . This indicates that the spin structure in the ordered phase of  $\text{Cs}_2\text{CuBr}_4$  is a helical incommensurate structure with ordering vector  $\mathbf{Q}_0 = (0, 0.575, 0)$ , similar to  $\text{Cs}_2\text{CuCl}_4$ .

Since the ordering vector is given by  $\cos(\pi Q_0) = -J_2/(2J_1)$ , we have  $J_2/J_1 = 0.467$  for  $\text{Cs}_2\text{CuBr}_4$ , which is 2.67 times as large as  $J_2/J_1 = 0.175$  for  $\text{Cs}_2\text{CuCl}_4$ . This implies that  $\text{Cs}_2\text{CuBr}_4$  is more frustrated than  $\text{Cs}_2\text{CuCl}_4$ . The magnetization curve for  $\text{Cs}_2\text{CuBr}_4$  was measured by Coldea *et al.*,<sup>19</sup> but the presence of the plateau has not been reported.

The magnetization curves for  $\text{Cs}_2\text{CuCl}_4$  and  $\text{Cs}_2\text{CuBr}_4$  have convex slopes below  $H_s$ . This behavior is characteristic of a low-dimensional antiferromagnet. However, the curvature of the convex slope for  $\text{Cs}_2\text{CuBr}_4$  is larger than that for  $\text{Cs}_2\text{CuCl}_4$ . This result suggests that the two dimensionality is better in  $\text{Cs}_2\text{CuBr}_4$  than in  $\text{Cs}_2\text{CuCl}_4$ . Thus we deduce that the magnitude of the interlayer exchange interaction is smaller than  $10^{-2} \times J_1$  also in  $\text{Cs}_2\text{CuBr}_4$ .

When the interlayer interaction and the small anisotropy energy are neglected, the saturation field  $H_s$  is given by

$$g\mu_B H_s = \{J(\mathbf{Q}_0) - J(0)\}S \\ = 2J_2\{1 - \cos(\pi Q_0)\} + J_1\{1 - \cos(2\pi Q_0)\}, \quad (1)$$

where  $J(\mathbf{Q})$  is the Fourier transform of the exchange interactions,<sup>22,23</sup> and is given by

$$J(\mathbf{Q}) = -4J_2 \cos(\pi Q) - 2J_1 \cos(2\pi Q) \quad (2)$$

for  $\mathbf{Q} = (0, Q, 0)$ . Here we define the exchange constant as  $\mathcal{H} = \sum_{(i,j)} J_{ij}(\mathbf{S}_i \cdot \mathbf{S}_j)$ . Inserting  $Q_0 = 0.575$ ,  $J_2/J_1 = 0.467$ , and  $gH_s \approx 63$  T obtained in the present measurements into Eq. (1), we obtain  $J_1/k_B = 27.8$  K and  $J_2/k_B = 13.0$  K.

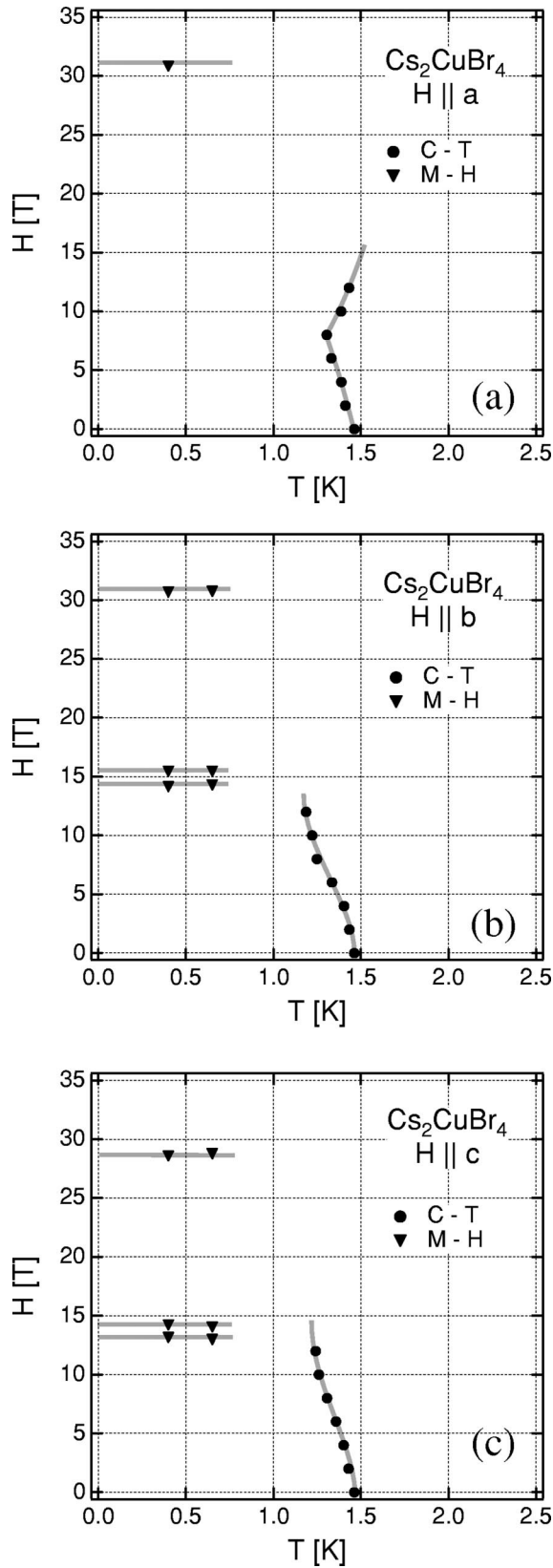


FIG. 8. Magnetic field vs temperature phase diagrams for  $\text{Cs}_2\text{CuBr}_4$  for (a)  $H \parallel a$ , (b)  $H \parallel b$ , and (c)  $H \parallel c$ . The gray lines are the guides for the eyes.

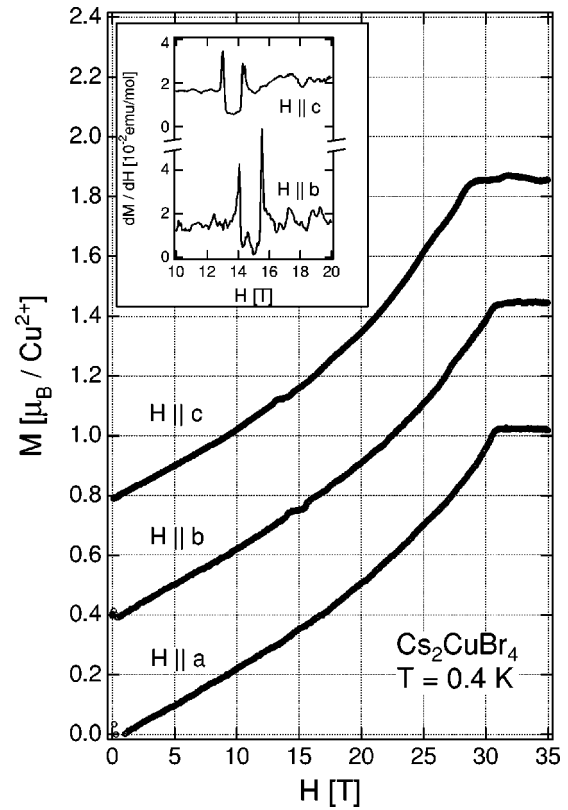


FIG. 9. Magnetization curves for  $\text{Cs}_2\text{CuBr}_4$  measured at  $T = 0.4$  K for  $H \parallel a$ ,  $H \parallel b$ , and  $H \parallel c$ . The values of the magnetization are shifted by  $0.4\mu_B$ . The inset shows  $dM/dH$  vs  $H$  around the magnetization plateau for  $H \parallel b$  and  $H \parallel c$ .

According to the classical molecular field theory,<sup>22,23</sup> a transition from a helical spin structure to a fan structure can occur when an external field is applied in the easy plane. The *helix-fan* transition is accompanied by a jump in magnetization, and not by the plateau. Examples of this include the recently observed phase transition in  $\text{RbCuCl}_3$  for a magnetic field perpendicular to the  $c$  axis.<sup>24,26</sup> At low temperatures,  $\text{RbCuCl}_3$  has a monoclinic structure, which is closely related to the crystal structure of  $\text{CsCuCl}_3$ .<sup>27,28</sup> The exchange interaction along the  $c$  axis is ferromagnetic, and interactions

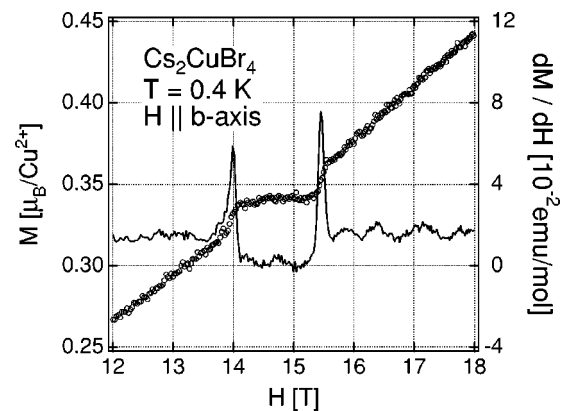


FIG. 10. The magnetization curve and  $dM/dH$  vs  $H$  for  $H \parallel b$  measured in magnetic fields up to 20 T.

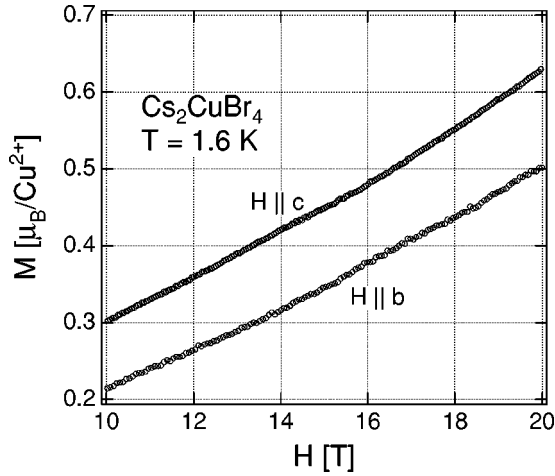


FIG. 11. The magnetization curves for  $H\parallel b$  and  $H\parallel c$  measured at  $T = 1.6$  K. The values of magnetization are shifted by  $0.1 \mu_B$ .

in the  $c$  plane are antiferromagnetic, as observed in  $\text{CsCuCl}_3$ . Due to the crystal distortion which breaks the hexagonal symmetry, the exchange network in the  $c$ -plane in  $\text{RbCuCl}_3$  is described by the same model as shown in Fig. 3(b). For this reason,  $\text{RbCuCl}_3$  has an incommensurate helical spin structure characterized by ordering vector  $\mathbf{Q}_0 = (0, 0.5985, 0)$  below  $T_N \approx 19$  K.<sup>29</sup> The helical spin structure in the  $c$ -plane is similar to those observed in  $\text{Cs}_2\text{CuBr}_4$  and  $\text{Cs}_2\text{CuCl}_4$ . In  $\text{RbCuCl}_3$ , no field-induced phase transition is observed for  $H\parallel c$ , in contrast to  $\text{CsCuCl}_3$ . In  $\text{RbCuCl}_3$ , the quantum fluctuation appears to be less important.

In the classical Heisenberg TAF with easy axis anisotropy, a magnetization plateau can exist at  $M_s/3$  when an external field is applied along the easy axis.<sup>30</sup> In the plateau region, the collinear  $uud$  spin structure along the magnetic field is stabilized by the easy-axis anisotropy. However, the magnetization curve has no plateau when an external field is perpendicular to the easy axis. The plateaus due to this classical mechanism have been observed in  $\text{RbFe}(\text{MoO}_4)_2$  and  $\text{CsFe}(\text{SO}_4)_2$  with  $S = \frac{5}{2}$ ,<sup>31</sup> and  $\text{GdPd}_2\text{Al}_3$  with  $S = \frac{7}{2}$ .<sup>32</sup>

In the classical 2D Heisenberg or  $XY$  TAF, the thermal fluctuation can stabilize the  $uud$  spin structure.<sup>33–35</sup> Consequently, the magnetization curve can have a plateau at  $M_s/3$ . However, the plateau is smeared and not completely flat due to the finite temperature effect. With decreasing temperature, the field range of the plateau decreases and vanishes at  $T = 0$ , because the thermal fluctuation is reduced.

Since the magnetization plateau in  $\text{Cs}_2\text{CuBr}_4$  is clearly observed for two different field directions at  $T = 0.4$  K, which is much lower than  $T_N = 1.4$  K, the plateau cannot be interpreted in terms of the classical model. Thus the magnetization plateau should be attributed to the quantum effect. As mentioned in Sec. I, in the  $S = \frac{1}{2}$  Heisenberg TAF, the quantum fluctuation removes the continuous degeneracy of the ground state spin configuration in the magnetic field, which is not possible in the classical approach, and stabilizes the  $uud$  spin structure in the finite field range to produce a plateau at  $M_s/3$ .<sup>2–6</sup> In the 2D TAF, the plateau is more enhanced, because the quantum fluctuation is more effective in 2D TAF than in 3D TAF. Since the magnetic properties of

$\text{Cs}_2\text{CuBr}_4$  may be described by the  $S = \frac{1}{2}$  quasi-2D distorted Heisenberg TAF, similarly to  $\text{Cs}_2\text{CuCl}_4$ , we infer that a magnetization plateau is produced by the mechanism similar to that for the spin- $\frac{1}{2}$  Heisenberg TAF. Therefore, we suggest that in the present system, the  $uud$  spin structure or closely related structure is realized at the plateau with the help of the quantum fluctuation.

The magnetization processes for  $H\parallel b$  and  $H\parallel c$  are almost the same. This result indicates that the spin configurations in magnetic fields for both the field directions are almost the same. Thus we can deduce that the magnetic anisotropy in the present system may be of the easy-plane type to confine spins in the  $bc$  plane, similarly to  $\text{Cs}_2\text{CuCl}_4$ . The possible origin of the anisotropy is the anisotropic exchange interaction of the form  $\Delta J S_i^x S_j^z$  and the dipole-dipole interaction. The magnitude of  $\Delta J$  could not be evaluated within the present measurements. ESR measurements are needed, because  $\Delta J$  can be evaluated from the zero-field gap of the ESR modes in the ordered state as has been done in  $\text{CsCuCl}_3$ <sup>25</sup> and  $\text{RbCuCl}_3$ .<sup>24</sup>

The classical magnetic susceptibility for  $H$  perpendicular to the helical plane is somewhat larger than that for  $H$  parallel to the helical plane except for the  $120^\circ$  structure for  $J_1 = J_2$ .<sup>23</sup> Thus the umbrella structure illustrated in Fig. 1(d) is stable for  $J_1 \neq J_2$ . The anisotropy of the easy-plane type does not prefer the collinear  $uud$  structure along the  $a$  axis. We infer that in the present system, the difference between the total classical energy for the umbrella structure and those for the structures illustrated in Figs. 1(a)–(c) overcome the difference between the quantum fluctuation energies for the latter structures and that for the umbrella structure, so that the magnetization plateau for  $H\parallel a$  is absent.

As seen in Figs. 9 and 10, the transition between the slope region and the plateau region appears to be of the first order. This suggests that the ordering vector  $\mathbf{Q}_0$  varies discontinuously at the transition field. As previously mentioned, the spin structure for  $H < H_{c1}$  was found to be a helical incommensurate structure and ordering vector is given by  $\mathbf{Q}_0 = (0, 0.575, 0)$  at zero field.<sup>21</sup> We infer that in the plateau state, the spin structure is locked into the collinear  $uud$  structure. The spin structure  $H_{c1} < H < H_s$  may be an incommensurate fan structure.<sup>26</sup> Therefore, we suggest that the successive *helix- $uud$ -fan* transition occurs with increasing magnetic field for  $H\parallel b$  and  $H\parallel c$ . Recently, Jacobs and Nikuni<sup>26</sup> commented on the possibility of this transition scenario. It is of great interest to investigate the magnetic field dependence of the ordering vector and spin configuration by neutron scattering.

Coldea and co-workers<sup>17,18</sup> obtained the magnetic field versus temperature diagram for  $\text{Cs}_2\text{CuCl}_4$ . They showed that for  $H\parallel c$ , the ordered phase vanishes before reaching saturation, and that the spin state between the ordered state and the saturated state is a spin liquid, while the phase boundary for  $H\parallel a$  is continuously connected to saturation and there is no anomaly on the phase boundary. In  $\text{Cs}_2\text{CuBr}_4$ , the phase transition was clearly observed up to 12 T, irrespective of the magnetic field direction. In order to check the presence of the ordered phase for  $H > 12$  T, specific heat measurements in

high magnetic fields are necessary. As shown in Fig. 8, the phase boundary for  $H\parallel a$  exhibits the bend anomaly at  $(T_m, H_m) = (1.3 \text{ K}, 8 \text{ T})$ . This behavior suggests that the point  $(T_m, H_m)$  is a multicritical point at which several phase boundaries meet. However, the anomaly indicative of the additional phase transition was not observed in the present measurement. Precise measurements around  $(T_m, H_m)$  are needed.

#### IV. CONCLUSIONS

We have presented the results of magnetization and specific heat measurements on the frustrated quantum spin system  $\text{Cs}_2\text{CuBr}_4$ . This compound undergoes magnetic ordering at  $T_N = 1.4 \text{ K}$  at zero magnetic field. The magnetic field dependence of the ordering temperature was investigated up to 12 T for three different field directions, and the results were

summarized in Fig. 8. The magnetization plateau was observed at approximately one-third of the saturation magnetization for  $H\parallel b$  and  $H\parallel c$ , while no plateau was observed for  $H\parallel a$ . The plateau should be attributed to the interplay of spin frustration and quantum fluctuation. The transition to the plateau state appears to be of the first order. We suggest that the successive *helix-uid-fan* transition occurs, with increasing magnetic field for  $H\parallel b$  and  $H\parallel c$ .

#### ACKNOWLEDGMENTS

The authors would like to thank T. Sakai, S. Miyashita, and T. Nikuni for useful comments on the magnetization plateau. This work was supported by Toray Science Foundation and a Grant-in-Aid for Scientific Research on Priority Areas (B) from the Ministry of Education, Culture, Sports, Science and Technology of Japan.

\*Electronic address: o-toshio@lee.phys.titech.ac.jp

†Electronic address: tanaka@lee.phys.titech.ac.jp

<sup>1</sup>M. F. Collins and O. A. Petrenko, *Can. J. Phys.* **75**, 605 (1997), and references therein.

<sup>2</sup>T. Nikuni and H. Shiba, *J. Phys. Soc. Jpn.* **62**, 3268 (1993).

<sup>3</sup>A. E. Jacobs, T. Nikuni, and H. Shiba, *J. Phys. Soc. Jpn.* **62**, 4066 (1993).

<sup>4</sup>H. Nishimori and S. Miyashita, *J. Phys. Soc. Jpn.* **55**, 4448 (1986).

<sup>5</sup>A. V. Chubukov and D. I. Golosov, *J. Phys.: Condens. Matter* **3**, 69 (1991).

<sup>6</sup>A. Honecker, *J. Phys.: Condens. Matter* **11**, 4697 (1999).

<sup>7</sup>H. Nojiri, Y. Tokunaga, and M. Motokawa, *J. Phys. (Paris), Colloq.* **49**, C8-1459 (1988).

<sup>8</sup>M. Motokawa, M. Arai, H. Ohta, M. Mino, H. Tanaka, and K. Ubukata, *Physica B* **211**, 199 (1995).

<sup>9</sup>U. Schotte, N. Stüßer, K. D. Schotte, H. Weinfurter, H. M. Mayer, and M. Winkelmann, *J. Phys.: Condens. Matter* **6**, 10 105 (1994).

<sup>10</sup>K. Adachi, N. Achiwa, and M. Mekata, *J. Phys. Soc. Jpn.* **49**, 545 (1980).

<sup>11</sup>N. V. Fedoseeva, R. S. Gekht, T. A. Velikanova, and A. D. Balaev, *Pis'ma Zh. Éksp. Teor. Fiz.* **41**, 332 (1985) [*JETP Lett.* **41**, 406 (1985)].

<sup>12</sup>H. B. Weber, T. Werner, J. Wosnitzer, H. von Löhneysen, and U. Schotte, *Phys. Rev. B* **54**, 15 924 (1996).

<sup>13</sup>B. Morosin and E. C. Lingafelter, *Acta Crystallogr.* **13**, 807 (1960).

<sup>14</sup>T. I. Li and G. D. Stucky, *Inorg. Chem.* **12**, 441 (1973).

<sup>15</sup>R. L. Carlin, R. Burriel, F. Palacio, R. A. Carlin, S. F. Keij, and D. W. Carnegie, Jr., *J. Appl. Phys.* **57**, 3351 (1985).

<sup>16</sup>R. Coldea, D. A. Tennant, R. A. Cowley, D. F. McMorrow, B. Dorner, and Z. Tylczynski, *J. Phys.: Condens. Matter* **8**, 7473

(1996).

<sup>17</sup>R. Coldea, D. A. Tennant, A. M. Tsvelik, and Z. Tylczynski, *Phys. Rev. Lett.* **86**, 1335 (2001).

<sup>18</sup>R. Coldea, D. A. Tennant, R. A. Cowley, D. F. McMorrow, B. Dorner, and Z. Tylczynski, *Phys. Rev. Lett.* **79**, 151 (1997).

<sup>19</sup>R. Coldea, D. A. Tennant, K. Habicht, P. Smeibidl, C. Wolters, and Z. Tylczynski, *Phys. Rev. Lett.* **88**, 137203 (2002).

<sup>20</sup>The ordering vector  $Q = (0, 0.472, 0)$  given in Ref. 16 should be read as  $Q = (0, 0.528, 0)$ .

<sup>21</sup>T. Ono, K. Nakajima, A. Oosawa, Y. Koike, H. Tanaka, and K. Kakurai (unpublished).

<sup>22</sup>T. Nagamiya, K. Nagata, and Y. Kitano, *Prog. Theor. Phys.* **27**, 1253 (1962).

<sup>23</sup>T. Nagamiya, *Solid State Phys.* **20**, 305 (1967).

<sup>24</sup>S. Maruyama, H. Tanaka, Y. Narumi, K. Kindo, H. Nojiri, M. Motokawa, and K. Nagata, *J. Phys. Soc. Jpn.* **70**, 859 (2001).

<sup>25</sup>H. Tanaka, U. Schotte, and K. D. Schotte, *J. Phys. Soc. Jpn.* **61**, 1344 (1992).

<sup>26</sup>A. E. Jacobs and T. Nikuni, *Phys. Rev. B* **65**, 174405 (2002).

<sup>27</sup>W. J. Crama, *J. Solid State Chem.* **39**, 168 (1981).

<sup>28</sup>M. Harada, *J. Phys. Soc. Jpn.* **52**, 1646 (1983).

<sup>29</sup>M. Reehuis, R. Feyherm, U. Schotte, M. Meschke, and H. Tanaka, *J. Phys. Chem. Solids* **62**, 1139 (2001).

<sup>30</sup>S. Miyashita, *J. Phys. Soc. Jpn.* **55**, 3605 (1986).

<sup>31</sup>T. Inami, Y. Ajiro, and T. Goto, *J. Phys. Soc. Jpn.* **65**, 2374 (1996).

<sup>32</sup>H. Kitazawa, H. Suzuki, H. Abe, and G. Kido, *Physica B* **259-261**, 3890 (1999).

<sup>33</sup>H. Kawamura and S. Miyashita, *J. Phys. Soc. Jpn.* **54**, 4530 (1985).

<sup>34</sup>H. Kawamura, *J. Phys. Soc. Jpn.* **53**, 2452 (1984).

<sup>35</sup>D. H. Lee, J. D. Joannopoulos, J. W. Negele, and D. P. Landau, *Phys. Rev. Lett.* **52**, 433 (1984).